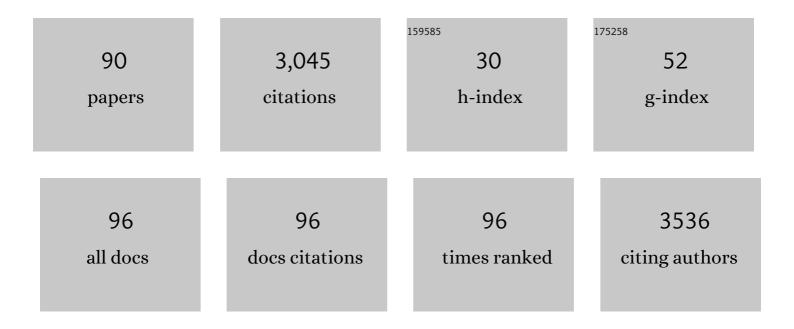
List of Publications by Year in descending order

Source: https://exaly.com/author-pdf/2147302/publications.pdf Version: 2024-02-01



#	Article	IF	CITATIONS
1	High Water Adsorption MOFs with Optimized Poreâ€Nanospaces for Autonomous Indoor Humidity Control and Pollutants Removal. Angewandte Chemie, 2022, 134, .	2.0	5
2	High Water Adsorption MOFs with Optimized Poreâ€Nanospaces for Autonomous Indoor Humidity Control and Pollutants Removal. Angewandte Chemie - International Edition, 2022, 61, .	13.8	42
3	A Rare Flexible Metal–Organic Framework Based on a Tailorable Mn <sub>8</sub> â€Cluster Showing Smart Responsiveness to Aromatic Guests and Capacity for Gas Separation. Angewandte Chemie - International Edition, 2022, 61, .	13.8	20
4	A Class of Readily Tunable Planar hiral Cyclopentadienyl Rhodium(III) Catalysts for Asymmetric C–H Activation. Angewandte Chemie - International Edition, 2022, 61, .	13.8	24
5	A Class of Readily Tunable Planar hiral Cyclopentadienyl Rhodium(III) Catalysts for Asymmetric C–H Activation. Angewandte Chemie, 2022, 134, .	2.0	2
6	A Rare Flexible Metal–Organic Framework Based on a Tailorable Mn <sub>8</sub> â€Cluster Showing Smart Responsiveness to Aromatic Guests and Capacity for Gas Separation. Angewandte Chemie, 2022, 134, .	2.0	2
7	Chiral Arene Ligand as Stereocontroller for Asymmetric Câ^'H Activation**. Angewandte Chemie - International Edition, 2022, 61, .	13.8	19
8	Pore-Nanospace Engineering of Mixed-Ligand Metal–Organic Frameworks for High Adsorption of Hydrofluorocarbons and Hydrochlorofluorocarbons. Chemistry of Materials, 2022, 34, 5116-5124.	6.7	11
9	Flexible Microporous Copper(II) Metal–Organic Framework toward the Storage and Separation of C1–C3 Hydrocarbons in Natural Gas. Inorganic Chemistry, 2021, 60, 8456-8460.	4.0	21
10	Qualitative screening and quantitative determination of multiclass water-soluble synthetic dyes in foodstuffs by liquid chromatography coupled to quadrupole Orbitrap mass spectrometry. Food Chemistry, 2021, 360, 129948.	8.2	14
11	Simultaneous determination of multiclass illegal dyes with different acidic–basic properties in foodstuffs by LC-MS/MS via polarity switching mode. Food Chemistry, 2020, 309, 125745.	8.2	24
12	A Flexible–Robust Copper(II) Metal–Organic Framework Constructed from a Fluorinated Ligand for CO <sub>2</sub> /R22 Capture. Inorganic Chemistry, 2020, 59, 14856-14860.	4.0	14
13	Frontispiz: A Voltageâ€Responsive Synthetic Cl <sup>â^'</sup> â€Channel Regulated by pH. Angewandte Chemie, 2020, 132, .	2.0	0
14	Progressive Folding and Adaptive Multivalent Recognition of Alkyl Amines and Amino Acids in p ‣ulfonatocalix[4]arene Hosts: Solid‣tate and Solution Studies. ChemPlusChem, 2020, 85, 1615-1615.	2.8	0
15	Frontispiece: A Voltageâ€Responsive Synthetic Cl <sup>â~'</sup> â€Channel Regulated by pH. Angewandte Chemie - International Edition, 2020, 59, .	13.8	0
16	Chiral Bicyclo[2.2.2]octaneâ€Fused CpRh Complexes: Synthesis and Potential Use in Asymmetric Câ°'H Activation. Angewandte Chemie, 2020, 132, 22622-22626.	2.0	38
17	Chiral Bicyclo[2.2.2]octaneâ€Fused CpRh Complexes: Synthesis and Potential Use in Asymmetric Câ^'H Activation. Angewandte Chemie - International Edition, 2020, 59, 22436-22440.	13.8	54

A Voltageâ€Responsive Synthetic Clâ^â€Channel Regulated by pH. Angewandte Chemie, 2020, 132, 19082-190882.0 3

#	Article	IF	CITATIONS
19	A Voltageâ€Responsive Synthetic Cl <sup>â^'</sup> â€Channel Regulated by pH. Angewandte Chemie - International Edition, 2020, 59, 18920-18926.	13.8	26
20	Progressive Folding and Adaptive Multivalent Recognition of Alkyl Amines and Amino Acids in <i>p</i> â€6ulfonatocalix[4]arene Hosts: Solidâ€6tate and Solution Studies. ChemPlusChem, 2020, 85, 1623-1631.	2.8	1
21	A New Class of <i>C</i> <sub>2</sub> â€5ymmetric Chiral Cyclopentadienyl Ligand Derived from Ferrocene Scaffold: Design, Synthesis and Application. Chemistry - A European Journal, 2020, 26, 14546-14550.	3.3	41
22	Rhodium(III) atalyzed Câ^'H/Nâ^'H Functionalization with Hydrogen Evolution. Chemistry - A European Journal, 2020, 26, 7365-7368.	3.3	4
23	Development of a <i>C</i> <sub>2</sub> -Symmetric Chiral <i>aza</i> Spirocyclic Diol. Organic Letters, 2020, 22, 3110-3113.	4.6	7
24	Rhodium(III)-Catalyzed Asymmetric C–H Activation of <i>N</i> -Methoxybenzamide with Quinone and Its Application in the Asymmetric Synthesis of a Dihydrolycoricidine Analogue. Organic Letters, 2020, 22, 3219-3223.	4.6	27
25	Dynamic Coordination Chemistry of Fluorinated Zrâ€MOFs: Synthetic Control and Reassembly/Disassembly Beyond de Novo Synthesis to Tune the Structure and Property. Chemistry - A European Journal, 2020, 26, 8254-8261.	3.3	16
26	Rücktitelbild: Selfâ€Assembled Columnar Triazole Quartets: An Example of Synergistic Hydrogenâ€Bonding/Anion–Ĩ€ Interactions (Angew. Chem. 35/2019). Angewandte Chemie, 2019, 131, 12434-12434.	2.0	0
27	All Roads Lead to Rome: Tuning the Luminescence of a Breathing Catenated Zr-MOF by Programmable Multiplexing Pathways. Chemistry of Materials, 2019, 31, 5550-5557.	6.7	30
28	Selfâ€Generation of Surface Roughness by Lowâ€6urfaceâ€Energy Alkyl Chains for Highly Stable Superhydrophobic/Superoleophilic MOFs with Multiple Functionalities. Angewandte Chemie - International Edition, 2019, 58, 17033-17040.	13.8	71
29	Innentitelbild: Whiteâ€Light Emission from Dualâ€Way Photon Energy Conversion in a Dyeâ€Encapsulated Metal–Organic Framework (Angew. Chem. 29/2019). Angewandte Chemie, 2019, 131, 9752-9752.	2.0	0
30	Selfâ€Generation of Surface Roughness by Lowâ€Surfaceâ€Energy Alkyl Chains for Highly Stable Superhydrophobic/Superoleophilic MOFs with Multiple Functionalities. Angewandte Chemie, 2019, 131, 17189-17196.	2.0	21
31	<i>N</i> -Methoxyamide: An Alternative Amidation Reagent in the Rhodium(III)-Catalyzed C–H Activation. Organic Letters, 2019, 21, 9315-9319.	4.6	28
32	Record high cationic dye separation performance for water sanitation using a neutral coordination framework. Journal of Materials Chemistry A, 2019, 7, 4751-4758.	10.3	44
33	How Does Azo Bond Cleave in the Gas Phase? Computational and Experimental Study on the Fragmentation Mechanism of Protonated Sudan I. ChemistrySelect, 2019, 4, 1666-1672.	1.5	3
34	Embedding CoO nanoparticles in a yolk–shell N-doped porous carbon support for ultrahigh and stable lithium storage. Journal of Materials Chemistry A, 2019, 7, 4036-4046.	10.3	46
35	Selfâ€Assembled Columnar Triazole Quartets: An Example of Synergistic Hydrogenâ€Bonding/Anion–π Interactions. Angewandte Chemie - International Edition, 2019, 58, 12037-12042.	13.8	14
36	Three-Component Synthesis of Isoquinoline Derivatives by a Relay Catalysis with a Single Rhodium(III) Catalyst. Organic Letters, 2019, 21, 4971-4975.	4.6	30

#	Article	IF	CITATIONS
37	Selfâ€Assembled Columnar Triazole Quartets: An Example of Synergistic Hydrogenâ€Bonding/Anion–π Interactions. Angewandte Chemie, 2019, 131, 12165-12170.	2.0	9
38	Whiteâ€Light Emission from Dualâ€Way Photon Energy Conversion in a Dyeâ€Encapsulated Metal–Organic Framework. Angewandte Chemie - International Edition, 2019, 58, 9752-9757.	13.8	145
39	Whiteâ€Light Emission from Dualâ€Way Photon Energy Conversion in a Dyeâ€Encapsulated Metal–Organic Framework. Angewandte Chemie, 2019, 131, 9854-9859.	2.0	21
40	Stable fluorinated 3D isoreticular nanotubular triazole MOFs: synthesis, characterization and CO2 separation. Journal of Porous Materials, 2019, 26, 1573-1579.	2.6	2
41	Enantioselective Synthesis of Câ`'N Axially Chiral Nâ€Aryloxindoles by Asymmetric Rhodium atalyzed Dual Câ`'H Activation. Angewandte Chemie - International Edition, 2019, 58, 6732-6736.	13.8	161
42	Enantioselective Synthesis of Câ^'N Axially Chiral Nâ€Aryloxindoles by Asymmetric Rhodium atalyzed Dual Câ^'H Activation. Angewandte Chemie, 2019, 131, 6804-6808.	2.0	63
43	Cobalt (oxy)hydroxide nanosheet arrays with exceptional porosity and rich defects as a highly efficient oxygen evolution electrocatalyst under neutral conditions. Journal of Materials Chemistry A, 2019, 7, 10217-10224.	10.3	23
44	Structural tuning of coordination polymers by 4-connecting metal node and secondary building process. Chinese Chemical Letters, 2019, 30, 1297-1301.	9.0	1
45	Introducing the Chiral Transient Directing Group Strategy to Rhodium(III) atalyzed Asymmetric Câ~'H Activation. Chemistry - A European Journal, 2019, 25, 4688-4694.	3.3	59
46	Unusual adsorption behaviours and responsive structural dynamics <i>via</i> selective gate effects of an hourglass porous metal–organic framework. RSC Advances, 2019, 9, 37222-37231.	3.6	3
47	A Flexible Cu-MOF as Crystalline Sponge for Guests Determination. Inorganic Chemistry, 2019, 58, 61-64.	4.0	22
48	A Metal–Organic Supramolecular Box as a Universal Reservoir of UV, WL, and NIR Light for Longâ€Persistent Luminescence. Angewandte Chemie - International Edition, 2019, 58, 3481-3485.	13.8	99
49	A Metal–Organic Supramolecular Box as a Universal Reservoir of UV, WL, and NIR Light for Longâ€Persistent Luminescence. Angewandte Chemie, 2019, 131, 3519-3523.	2.0	25
50	Catalysis through Dynamic Spacer Installation of Multivariate Functionalities in Metal–Organic Frameworks. Journal of the American Chemical Society, 2019, 141, 2589-2593.	13.7	98
51	Metal Effects on the Framework Stability and Adsorption Property of a Series of Isoreticular Metal–Organic Frameworks Based on an in-Situ Generated T-Shaped Ligand. Crystal Growth and Design, 2019, 19, 300-304.	3.0	8
52	Framework disorder and its effect on selective hysteretic sorption of a T-shaped azole-based metal–organic framework. IUCrJ, 2019, 6, 85-95.	2.2	10
53	Probing of the supramolecular interaction between anti-cancer drug carmofur and a Zn4L4 metal-organic cage in acetonitrile. Inorganic Chemistry Communication, 2018, 87, 24-26.	3.9	3
54	Tunability of fluorescent metal–organic frameworks through dynamic spacer installation with multivariate fluorophores. Chemical Communications, 2018, 54, 13666-13669.	4.1	22

#	Article	IF	CITATIONS
55	Design and Enantioresolution of Homochiral Fe(II)–Pd(II) Coordination Cages from Stereolabile Metalloligands: Stereochemical Stability and Enantioselective Separation. Journal of the American Chemical Society, 2018, 140, 18183-18191.	13.7	102
56	Asymmetric Rh(I)-Catalyzed Functionalization of the 3-C( <i>sp</i> <sup>3</sup> )–H Bond of Benzofuranones with α-Diazoesters. Organic Letters, 2018, 20, 5889-5893.	4.6	24
57	Hierarchically Porous Single Nanocrystals of Bimetallic Metal–Organic Framework for Nanoreactors with Enhanced Conversion. Chemistry of Materials, 2018, 30, 6458-6468.	6.7	24
58	A facile method for scalable synthesis of ultrathin g-C <sub>3</sub> N <sub>4</sub> nanosheets for efficient hydrogen production. Journal of Materials Chemistry A, 2018, 6, 18252-18257.	10.3	40
59	A mesoporous metal-organic framework based on T-shape ligand with Ca2+ release behavior under simulated physiological conditions and praisable biocompatibility. Inorganic Chemistry Communication, 2018, 94, 1-4.	3.9	2
60	A Recoverable Complex with Nitrogenâ€Rich Double Rings for Hg(II) Sorption. ChemistrySelect, 2018, 3, 7592-7595.	1.5	3
61	A stable metal cluster-metalloporphyrin MOF with high capacity for cationic dye removal. Journal of Materials Chemistry A, 2018, 6, 17698-17705.	10.3	102
62	Investigation of Binding Behavior between Drug Molecule 5â€Fluoracil and M <sub>4</sub> L <sub>4</sub> â€Type Tetrahedral Cages: Selectivity, Capture, and Release. Chemistry - A European Journal, 2017, 23, 3542-3547.	3.3	28
63	A Robust Metal–Organic Framework Combining Open Metal Sites and Polar Groups for Methane Purification and CO <sub>2</sub> /Fluorocarbon Capture. Chemistry - A European Journal, 2017, 23, 4060-4064.	3.3	62
64	Dynamic Spacer Installation for Multirole Metal–Organic Frameworks: A New Direction toward Multifunctional MOFs Achieving Ultrahigh Methane Storage Working Capacity. Journal of the American Chemical Society, 2017, 139, 6034-6037.	13.7	168
65	Frontispiece: Investigation of Binding Behavior between Drug Molecule 5â€Fluoracil and M <sub>4</sub> L <sub>4</sub> â€Type Tetrahedral Cages: Selectivity, Capture, and Release. Chemistry - A European Journal, 2017, 23, .	3.3	1
66	A Porous Zn(II)-Metal–Organic Framework Constructed from Fluorinated Ligands for Gas Adsorption. Crystal Growth and Design, 2017, 17, 1476-1479.	3.0	25
67	Hydrophobic metallo-supramolecular Pd <sub>2</sub> L <sub>4</sub> cages for zwitterionic guest encapsulation in organic solvents. Dalton Transactions, 2017, 46, 15204-15207.	3.3	12
68	Stepwise engineering of pore environments and enhancement of CO <sub>2</sub> /R22 adsorption capacity through dynamic spacer installation and functionality modification. Chemical Communications, 2017, 53, 11403-11406.	4.1	22
69	Nanoparticle Cookies Derived from Metalâ€Organic Frameworks: Controlled Synthesis and Application in Anode Materials for Lithiumâ€Ion Batteries. Small, 2016, 12, 2365-2375.	10.0	96
70	Nanoreactor Based on Macroporous Single Crystals of Metal-Organic Framework. Small, 2016, 12, 5702-5709.	10.0	74
71	Ligand and Metal Effects on the Stability and Adsorption Properties of an Isoreticular Series of MOFs Based on Tâ€Shaped Ligands and Paddleâ€Wheel Secondary Building Units. Chemistry - A European Journal, 2016, 22, 16147-16156.	3.3	43
72	Precise Modulation of the Breathing Behavior and Pore Surface in Zrâ€MOFs by Reversible Post‣ynthetic Variable‣pacer Installation to Fineâ€Tune the Expansion Magnitude and Sorption Properties. Angewandte Chemie, 2016, 128, 10086-10090.	2.0	30

#	Article	IF	CITATIONS
73	Precise Modulation of the Breathing Behavior and Pore Surface in Zrâ€MOFs by Reversible Postâ€Synthetic Variableâ€Spacer Installation to Fineâ€Tune the Expansion Magnitude and Sorption Properties. Angewandte Chemie - International Edition, 2016, 55, 9932-9936.	13.8	125
74	Cp*Co <sup>III</sup> -Catalyzed C–H Alkenylation/Annulation to Afford Spiro Indenyl Benzosultam. Journal of Organic Chemistry, 2016, 81, 6093-6099.	3.2	56
75	Solvent- and anion-induced interconversions of metal–organic cages. Chemical Communications, 2016, 52, 8745-8748.	4.1	31
76	Face apped M <sup>4</sup> L <sub>4</sub> Tetrahedral Metal–Organic Cage: lodine Capture and Release, Ion Exchange, and Electrical Conductivity. Chemistry - an Asian Journal, 2016, 11, 216-220.	3.3	23
77	Time controlled structural/packing transformation and tunable luminescence of Cd(ii)-chloride-triBZ-ntb coordination assemblies: an experimental and theoretical exploration. CrystEngComm, 2015, 17, 546-552.	2.6	17
78	Structural transition between a (4,4)-net and a Cdl2-net in Cd(II) compounds and conversion from a mixture to a pure substance. Inorganic Chemistry Communication, 2015, 55, 116-119.	3.9	19
79	Semidirected versus holodirected coordination and single-component white light luminescence in Pb( <scp>ii</scp> ) complexes. New Journal of Chemistry, 2015, 39, 5287-5292.	2.8	36
80	Assembly of BF <sub>4</sub> <sup>â^'</sup> , PF <sub>6</sub> <sup>â^'</sup> , ClO <sub>4</sub> <sup>â^'</sup> and F <sup>â^'</sup> with trinuclear copper( <scp>i</scp> ) acetylide complexes bearing amide groups: structural diversity, photophysics and anion binding properties. RSC Advances, 2015, 5, 89669-89681.	3.6	15
81	Amide and N-oxide functionalization of T-shaped ligands for isoreticular MOFs with giant enhancements in CO <sub>2</sub> separation. Chemical Communications, 2014, 50, 14631-14634.	4.1	107
82	Structural disorder and transformation in crystal growth: direct observation of ring-opening isomerization in a metal–organic solid solution. IUCrJ, 2014, 1, 318-327.	2.2	16
83	Assembly of Ag(i) coordination polymers from a tripyridyl-ester ligand: effects of counter anion, ligand conformation and ï€â€"ï€ interaction on non-interpenetrating 2D → 3D dimension increase. CrystEngComm, 2013, 15, 9751.	2.6	8
84	Porous zinc(II)-organic framework with potential open metal sites: Synthesis, structure and property. Science China Chemistry, 2011, 54, 1436-1440.	8.2	13
85	1â€Dâ€Tin(II) Phenylchalcogenolato Complexes <sub>â^ž</sub> <sup>1</sup> [Sn(EPh) <sub>2</sub> ] (E = S, Se Inorganic Chemistry, 2010, 2010, 410-418.	.) Tj ETQq 2.0	1 1 0.7843 25
86	Thermally Stable Porous Hydrogenâ€Bonded Coordination Networks Displaying Dual Properties of Robustness and Dynamics upon Guest Uptake. Chemistry - A European Journal, 2010, 16, 1841-1848.	3.3	72
87	Assembly of Robust and Porous Hydrogen-Bonded Coordination Frameworks: Isomorphism, Polymorphism, and Selective Adsorption. Inorganic Chemistry, 2010, 49, 10166-10173.	4.0	64
88	Self-Assembly of Triple Helical andmeso-Helical Cylindrical Arrays Tunable by Bis-Tripodal Coordination Converters. Inorganic Chemistry, 2008, 47, 10692-10699.	4.0	41
89	The interplay of coordinative and hydrogen-bonding in directing the [M(4,4′-bpy)2(H2O)2] square-grid networks: formation of 3D porous framework [Cd(4,4′-bpy)2(H2O)2](ClO4)2(4,4′-bpy)(CH3OH)2. CrystEngComm, 2008, 10, 1147.	2.6	19
90	A new Ag(i)–4,4′-bipyridine coordination polymer of honeycomb (6,3) networks containing a Ag6(4,4′-bipy)6 hexagonal ring of 17 × 26 à dimensions. CrystEngComm, 2005, 7, 603.	2.6	21